

## Mediterranean Marine Science

Vol 25, No 3 (2024)

Mediterranean Marine Science



### Pinna nobilis refugia breached: Ongoing Mass Mortality Event in the Gulf of Kalloni (Aegean Sea)

ATHANASIOS NIKOLAOU, EVANGELOS  
PAPADIMITRIOU, ELLI KIOURANI, STELIOS  
KATSANEVAKIS

doi: [10.12681/mms.38613](https://doi.org/10.12681/mms.38613)

#### To cite this article:

NIKOLAOU, A., PAPADIMITRIOU, E., KIOURANI, E., & KATSANEVAKIS, S. (2024). Pinna nobilis refugia breached: Ongoing Mass Mortality Event in the Gulf of Kalloni (Aegean Sea). *Mediterranean Marine Science*, 25(3), 747–752. <https://doi.org/10.12681/mms.38613>

## ***Pinna nobilis* refugia breached: Ongoing Mass Mortality Event in the Gulf of Kalloni (Aegean Sea)**

Athanasios NIKOLAOU, Evangelos PAPANIMITRIOU, Elli KIOURANI and Stelios KATSANEVAKIS

*Mediterranean Marine Science*, 25 (3) 2024

### **Detailed methodology of distance sampling**

Distance sampling is used to tackle imperfect detectability when estimating the density and abundance of a population (Buckland *et al.*, 1993). This is done by estimating the probability of detection  $\hat{P}_a$ , through fitting a model on the perpendicular distance data that describes the *detection function*  $g(y)$ . The *detection function* is the probability that an individual at distance  $y$  is recorded, given that  $g(0)=1$  meaning that all individuals on the transect line are recorded. To get an estimation of the density of the population, the probability of detection  $\hat{P}_a$  is estimated using the *detection function*  $g(y)$  as shown below

$$\hat{P}_a = \frac{\hat{\mu}}{w} \quad \text{Eq. 1}$$

Where  $\mu = \int_0^w g(y)dy$  is the estimated effective strip half-width and  $w$  is the strip half-width. The effective strip half-width is defined as the distance from the transect line at which the expected number of observations beyond the distance  $\mu$  equals the unrecorded individuals within  $\mu$  (Buckland *et al.*, 2015).

The population density of each sampling site ( $h$ ) can be written as shown below

$$\widehat{D}_h = \frac{n}{2wL\hat{P}_a} = \frac{n}{2\hat{\mu}L} \quad \text{Eq. 2}$$

Where  $n$  is the number of recorded individuals,  $L$  is the total length of the transects. By rescaling  $g(y)$  so that it integrates to one we derive the *probability density function*  $f(y)$ . Thus  $f(y)=g(y)/\mu$  for  $0 \leq y \leq w$ , because we assumed that  $g(0)=1$  the Eq. 2 can be written as:

$$\widehat{D}_h = \frac{nf(0)}{2L} \quad \text{Eq. 3}$$

The variance of  $\widehat{D}_h$  is estimated as:

$$\widehat{\text{var}}(\widehat{D}_h) = \widehat{D}_h^2 \left[ \frac{\widehat{\text{var}}(n)}{n^2} + \frac{\widehat{\text{var}}[\hat{f}(0)]}{[\hat{f}(0)]^2} \right] \quad \text{Eq. 4}$$

The variance of  $n$  is estimated from the sample variance in encounter rates  $\left(\frac{n_i}{l_i}\right)$ . Maximum likelihood theory is used to estimate  $\hat{f}(0)$  and subsequently its variance from the information matrix (Buckland *et al.*, 2001).

To model the *detection function* and thus estimate the population density, the Distance 7.5 release 2 software (Thomas *et al.*, 2010) was used. A set of candidate models were fitted to the data for the two sampling periods to estimate the *detection function* for live individuals. In total, 22 models were fitted using both conventional distance sampling (CDS) models and multiple covariate distance (MCDS) models (see Table S1 for the set of candidate models). Candidate models were fitted using two 'key' functions; Hazard rate and Half-normal, with various adjustments terms and covariates (habitat, visibility, and the shell width).

Model selection was based on Akaike's information criterion (AIC; Akaike, 1974). Additionally, the overall goodness-of-fit was examined using Kolmogorov-Smirnov and Cramer-von Mises tests (Burnham *et al.*, 2004).

## References

- Akaike, H., 1974. A new look at the statistical model identification. *IEEE transactions on automatic control*, 19 (6), 716-723.
- Buckland, S.T., Anderson, D.R., Burnham, K.P., Laake, J.L. 1993. *Distance Sampling: Estimating Abundance of Biological Populations*. Chapman and Hall, London. 446 pp.
- Buckland, S.T., Rexstad, E.A., Marques, T.A., Oedekoven, C.S., 2015. *Distance sampling: methods and applications* (Vol. 431). Springer, New York. 277 pp.
- Burnham, K.P., Buckland, S.T., Laake, J.L., Borchers, D.L., Marques, T.A., *et al.*, 2004. Further topics in distance sampling. p. 307-392. In: *Advanced Distance Sampling*. Buckland, S.T., Anderson, D.R., Burnham, K.P., Laake J.L., Brochers, D.L., Thomas, L. (Eds). Oxford University Press, Oxford.
- Thomas, L., Buckland, S.T., Rexstad, E.A., Laake, J.L., Strindberg, S. *et al.*, 2010. Distance software: design and analysis of distance sampling surveys for estimating population size. *Journal of Applied Ecology*, 47 (1), 5-14.

**Table S1.** Set of candidate models.

ID	Key function	Series expansion	Covariates
a1	Hazard rate	-	-
a2	Half normal	-	-
a3	Hazard rate	Cosine	-
a4	Hazard rate	Simple polynomial	-
a5	Hazard rate	Hermite polynomial	-
a6	Half normal	Cosine	-
a7	Half normal	Simple polynomial	-
a8	Half normal	Hermite polynomial	-
a9	Hazard rate	-	Habitat
a10	Hazard rate	-	Visibility
a11	Hazard rate	-	Width
a12	Hazard rate	-	Habitat and visibility
a13	Hazard rate	-	Visibility and width
a14	Hazard rate	-	Habitat and width
a15	Hazard rate	-	Habitat, visibility and width
a16	Half normal	-	Habitat
a17	Half normal	-	Visibility
a18	Half normal	-	Width
a19	Half normal	-	Habitat and visibility
a20	Half normal	-	Visibility and width
a21	Half normal	-	Habitat and width
a22	Half normal	-	Habitat, visibility and width

**Table S2.** Best models selected based on AIC and results of goodness of fit tests.

Best model	May/June	September/October
Model	a1	a18
Key function	Hazard rate	Half normal
Series expansion	-	-
Covariates	-	Width
K-S test	$p = 0.54$	$p = 0.73$
C-von M test (unweighted)	$p > 0.5$	$p > 0.7$
C-von M test (weighted)	$p > 0.4$	$p > 0.6$

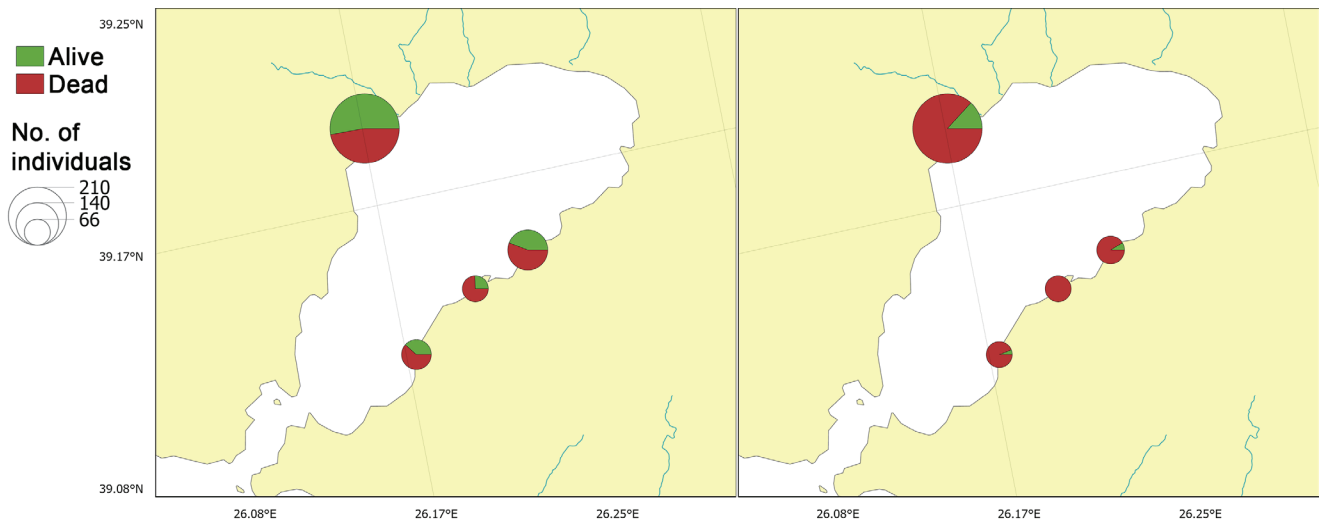


**Fig. S1:** Pie charts for each study site showing the number of live and dead individuals between May-June (left) and September-October (right). The size of each pie chart is proportional to the total number of individuals.